



Was Common Era glacier expansion in the Arctic Atlantic region triggered by unforced atmospheric cooling?

Willem G.M. van der Bilt ^{a, b,*}, Andreas Born ^{a, b}, Kristian A. Haaga ^{a, c}

^a Department of Earth Science, University of Bergen, Allégaten 41, 5007, Bergen, Norway

^b Bjerknes Centre for Climate Research, Bergen, Norway

^c K.G. Jebsen Centre for Deep Sea Research, Bergen, Norway



ARTICLE INFO

Article history:

Received 12 May 2019

Received in revised form

22 July 2019

Accepted 27 July 2019

Available online 5 August 2019

Keywords:

Little Ice Age

Late Holocene

Threshold response

Sea-ice feedbacks

Neoglacial

ABSTRACT

The timing and causes of Common Era (CE) glacier growth in the Arctic Atlantic region remain elusive. There is mounting evidence of advances that predate the Little Ice Age (1250–1850 CE); this challenges the view that 13th century volcanic eruptions triggered change by spurring sea-ice expansion. Recent climate model simulations indicate this response does not require external forcing under contemporaneous (Pre-Industrial) boundary conditions. Here, we try to reconcile these new insights by combining regional proxy evidence of glacier and sea-ice change with a climate model experiment. Collated recently published reconstructions demonstrate that regional climate shifted towards a colder mean state around 650–950 CE, a period marked by low radiative forcing. Unforced model simulations reproduce the time-transgressive evolution of this response, which emerged east of Greenland and progressed towards Svalbard. The inferred pattern is associated with sea-ice feedbacks, triggered by stochastic atmospheric cooling. We argue that this mechanism may explain the timing and pattern of CE glacier growth in the region.

© 2019 The Authors. Published by Elsevier Ltd. This is an open access article under the CC BY-NC-ND license (<http://creativecommons.org/licenses/by-nc-nd/4.0/>).

1. Introduction

The Little Ice Age (LIA) marks the most recent and well-known phase of Holocene climate deterioration (Liu et al., 2014), and holds valuable insights to help understand thresholds and feedbacks in the natural climate system. LIA change was most pronounced in the Northern Hemisphere (e.g. Mann et al., 2009), where glaciers advanced towards their post-glacial maxima. Compilations of reconstructed mid-latitude (40–60°N) glacier change generally propose an onset around 1300 CE, followed by ice expansion until ~1850 CE (Solomina et al., 2016).

However, a rapidly expanding body of recent work suggests that glaciers in the Arctic Atlantic region (65–80°N; Fig. 1) started advancing centuries prior to the classical (1250–1850 CE; IPCC, 2001) LIA (e.g. Balascio et al., 2015; Larsen et al., 2017; Miller et al., 2013; Philipp et al., 2017; Schweinsberg et al., 2017; Young et al., 2015), set against a background of regional summer cooling (Werner et al., 2018). This evidence challenges the commonly held

view that Common Era (CE) glacier growth was driven by negative radiative forcing from a series of volcanic eruptions during a time of low solar activity around 1250 CE, and amplified by sea-ice feedbacks (e.g. Hormes et al., 2006; Miller et al., 2012). Indeed, timing of regional glacier growth is often coincident with the Medieval Warm (and Quiet) Periods (MWP; 950–1250 CE, MQP; 725–1025 CE), a time characterized by stable radiative forcing (Bradley et al., 2016; Mann et al., 2009).

Simulations from recent (generation CMIP5) coupled climate models suggest that similar sea-ice feedbacks may arise spontaneously (unforced) under similar (Pre-Industrial) boundary conditions (Drijfhout et al., 2013; Kleppin et al., 2015). In such a scenario, stochastic sea level pressure anomalies east of Greenland initiate a positive feedback loop of surface cooling and sea-ice expansion across the Arctic Atlantic that could become self-sustained (Lehner et al., 2013).

Here, we assess whether this mechanism can explain the timing and pattern of CE Arctic Atlantic glacier growth. To do so, we compare selected recent well-dated reconstructions of regional glacier and sea-ice variability to climate model output. Our synthesis identifies a diachronous phase of rapid glacier and sea-ice growth that shifted Arctic Atlantic climate towards a cooler mean

* Corresponding author. Department of Earth Science, University of Bergen, Allégaten 41, 5007, Bergen, Norway.

E-mail address: willevanderbilt@uib.no (W.G.M. van der Bilt).

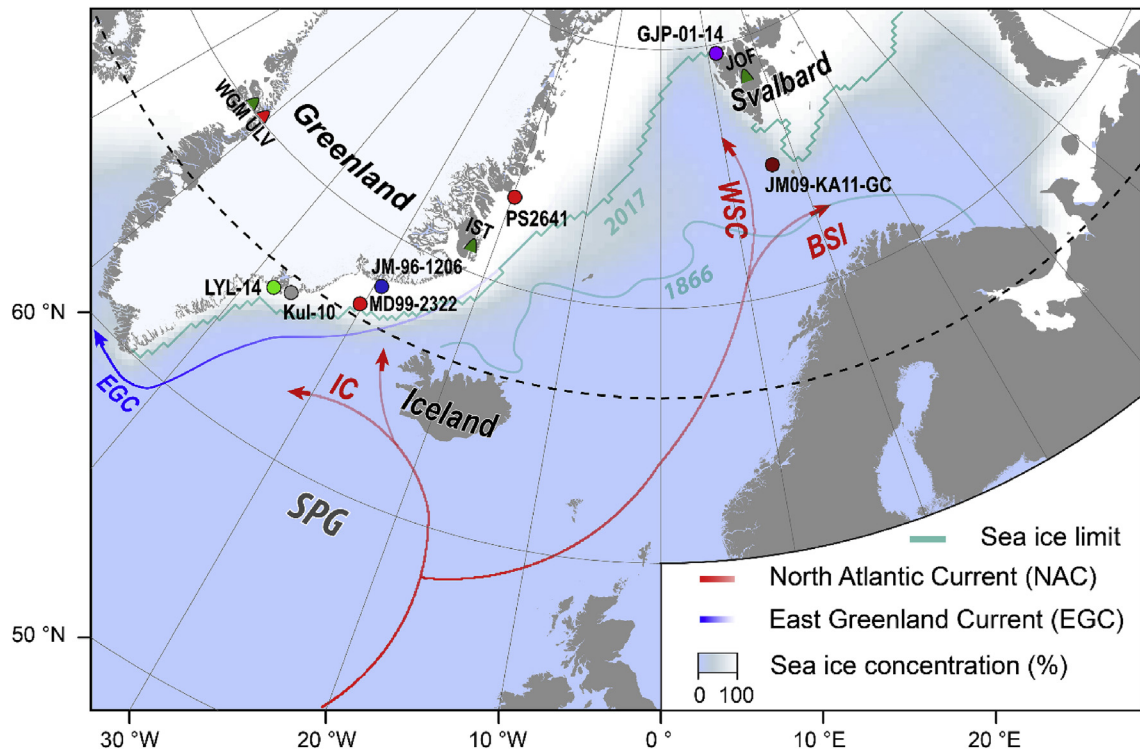


Fig. 1. Overview map of the Arctic Atlantic region. White shading highlights average 1972–2007 CE sea-ice concentrations after Fetterer et al. (2016). Minimal (2017 CE) and maximum (1866 CE; Divine and Dick, 2006) observed March sea-ice maxima are marked in turquoise. Blue and red lines indicate polar and Atlantic currents, respectively, marking the Subpolar Gyre (SPG), Irminger Current (IC), East Greenland Current (EGC), West Spitsbergen Current (WSC) and Barents Sea Inflow (BSI). Circles mark discussed sediment records, shown in matching colors in Figs. 2–3. LYL-14 and Kul-10 from the glacier-fed Ymer and Kulusuk lakes on Ammassalik archipelago (Balascio et al., 2015; van der Bilt et al., 2018). GJP-01-14 from glacier-fed Gjøavatnet on NW Svalbard (De Wet et al., 2017), JM09-KA11-GC from the W Barents Sea margin (Berben et al., 2014), as well as JM-96-1206, MD99-2322 and PS2641 from the E Greenland shelf (Andrews et al., 2016; Kolling et al., 2017; Perner et al., 2016; Miettinen et al., 2015). Green and red triangles, respectively, mark sample sites of ice-entombed moss and cosmogenic moraine ages in Fig. 2. IST – Istvortet (Lowell et al., 2013; Miller et al., 2013), MT – Mittivakkat (Hasholt, 2000), WGM - W Greenland moss chronology (Schweinsberg et al., 2017), ULV - Uigordleq Lake Valley (Young et al., 2015) and JOF – Jotunfonna (Miller et al., 2017). (For interpretation of the references to color in this figure legend, the reader is referred to the Web version of this article.)

state between ~650 and 950 CE. Timing of this climate deterioration during a period with little volcanism and stable solar activity does not favor a radiative trigger, while the time-transgressive pattern of change is consistent with model evidence of stochastic atmospheric cooling. Our findings help reconcile empirical evidence of pre-LIA glacier growth with simulations of unforced cooling, and underscores the importance of sea-ice feedbacks as catalysts of Late Holocene change.

2. Methods

Our main aim is to assess whether unforced sea-ice feedbacks could have triggered pre-LIA glacier expansion across the North Atlantic Arctic. This coupled response has often been invoked to explain reconstructed glacier change in the region (Cabedo-Sanz et al., 2016; Larsen et al., 2013). We validate this conceptual framework by correlating observations of regional summer (melting season) temperature and sea-ice extent (Fig. 1; 60–90°N, 50°W–20°E) (Divine and Dick, 2006; Morice et al., 2012), against proxy-based evidence of historical glacier variability. To this end, we rely on the lake-based glacier reconstructions from Ammassalik Archipelago on E Greenland by van der Bilt et al. (2018) and Balascio et al. (2015) for two reasons. First, their ability to capture historical (post-1850 CE) variability in unprecedented detail; both records derive from highly responsive small ($<1 \text{ km}^2$) glaciers that respond to change with a negligible lag (Bahr et al., 1998), and harness the potential of lead (^{210}Pb) dating to constrain this response on decadal timescales. Secondly, the exceptional sensitivity of the

Ammassalik area to regional climate change. Situated near the seasonal sea-ice margin and the interface of Arctic (East Greenland Current; EGC) and Atlantic (Irminger Current; IC) waters (Fig. 1), observations reveals record-setting changes in surface (ocean) temperatures, sea-ice conditions and glacier extent (Andresen et al., 2012; Bjørk et al., 2012; Straneo et al., 2010). Moreover, and of key relevance to this study, simulated unforced cooling events under CE (Pre-Industrial) boundary conditions consistently emerge E of Greenland (Drijfhout et al., 2013; Kleppin et al., 2015). We calculated correlation coefficients on evenly interpolated 5-year moving averages using Spearman's rho (ρ).

To assess the timing and pattern of Arctic Atlantic glacier expansion during the CE and its links to sea-ice change, we collate a selection of recent regional reconstructions that resolve variability on centennial-time scales and provide age ties for major transitions. With the exception of Balascio et al. (2015), none of these records were included in recent reviews on Late Holocene cooling and glacier growth by McKay et al. (2018) and Solomina et al. (2016). We combine three lines of regional paleoglaciological evidence from the region (Fig. 1). First, moraine exposure dates, which mark the culmination of glacier advances (e.g. Young et al., 2015). Secondly, vegetation kill dates, constraining the expansion of non-erosive ice (e.g. Miller et al., 2017). Finally, glaciogenic lake sediment input, providing snapshots of past ice margin positions (threshold lakes; e.g. Larsen et al., 2017), or recording continuous variations of alpine glaciers (distal glacier-fed lakes; e.g. Bakke et al., 2009). Our synthesis only includes records that derive from small ($<100 \text{ km}^2$) glaciers or ice caps, because of their rapid (decadal-scale) response

to climate perturbations (Bahr et al., 1998). We exclude records from areas with reported occurrence of carbonate-holding bedrock (e.g. Levy et al., 2014; van der Bilt et al., 2015), which could introduce chronological uncertainty because of freshwater reservoir effects. Finally, additional analyses were performed on the LYL-14 record from Ymer Lake by van der Bilt et al. (2018) (Fig. 1). We doubled the sampling resolution to acquire 5 cm down-core resolution for the past 1.5 ka to pinpoint the onset of silt-dominated glaciogenic sedimentation (Leemann and Niessen, 1994). For this purpose, we used a Malvern Mastersizer 3000 following removal of organic material with 35% v/v H₂O₂.

To assess leads and lags between the selected sediment archives from the Arctic Atlantic region (Fig. 1), the timing of maximum CE proxy change was calculated after Bernhardt et al. (2017). To do so, we remodeled all chronologies following specifications outlined in the original publications, using the mean values and 95% confidence bands of age distributions. Differences in dating resolution were negated by interpolating time series at 1 yr intervals, smoothing them with a 100-yr Gaussian filter and placing data into equidistant 50–150 yr bins using 2 yr steps. Additional statistical analyses include the calculation of weighted mean proxy values and their standard deviations (1σ) for the Late Holocene (past 4.2 ka) to contextualize the magnitude of CE change. Finally, we used the rcarbon R Package by Bevan et al. (2018) to calculate the cumulative age distribution of sets of published vegetation kill dates and moraine ages.

To compare collated proxy evidence with model evidence of unforced climate deterioration under CE boundary conditions, we use a published simulation that was run with version 2.2 of EC-Earth 2.2 (Hazeleger et al., 2012; model description in Supplementary Materials). We analyzed a pre-industrial control run, conducted by the Irish Meteorological Service (Met Éireann), and previously published by Drijfhout et al. (2013). This simulation was run for 1125 yrs and initialized using observations from the 2001 World Ocean Atlas and ERA-40 re-analysis of January 1, 1979. Greenhouse gas and aerosol concentrations were kept at pre-industrial (PI; 1850 CE) levels. Our analysis focuses on a cold event that emerges 390 years into the run and culminates between 450 and 550 years. We compare Surface Air Temperature (SAT) and Sea Ice Concentration (SIC) change to the 200–390 years reference PI climate state defined by Drijfhout et al. (2013).

3. Results and discussion

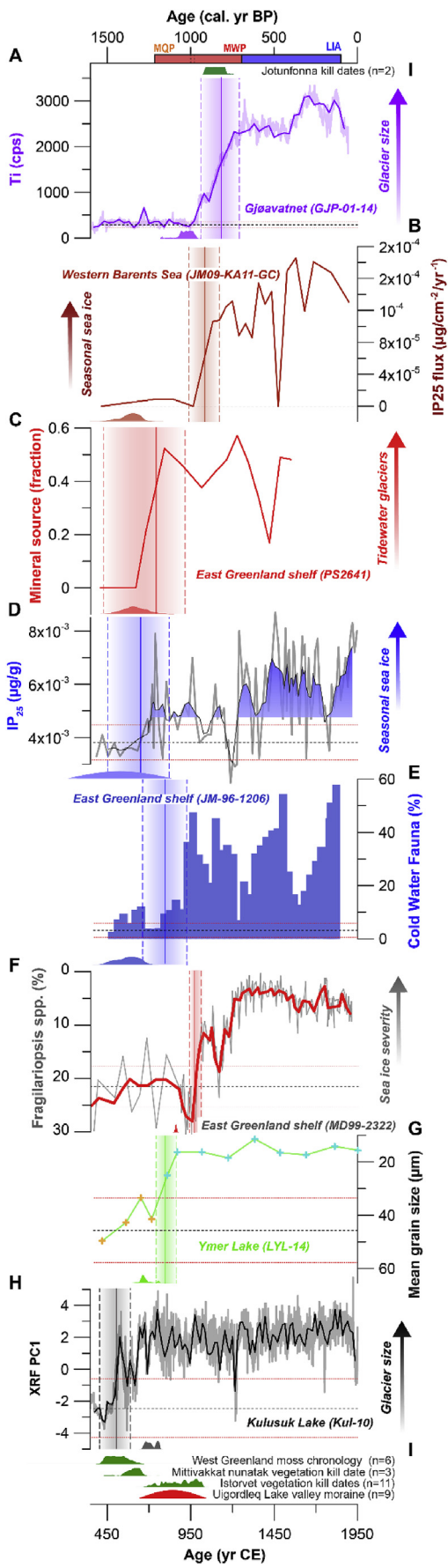
As seen in Fig. 2, the period around 750 CE is characterized by widespread expansion of glaciers and small ice caps on Greenland. Additional grain size analyses allow us to refine the timing of Ymer glacier reformation to ~810 CE (Fig. 2g), when sample grain size distribution shifts an order of magnitude towards a mode in the silt fraction that dominates glaciogenic input (Leemann and Niessen, 1994). The probability density function of ^{14}C ages from plants killed by overriding ice suggests that the adjacent Mittivakkat glacier advanced after ~650 CE (Figs. 1 and 2i; Hasholt, 2000). Based on the same approach, summed probability distributions of dated entombed mosses indicate that small ice caps on W (WGM) and E Greenland (Istorvet; IST) started expanding by 650 CE and 950 CE, respectively (Figs. 1 and 2i; Miller et al., 2013; Schweinsberg et al., 2017). A prompt increase in the terrigenous mineral content of E Greenland shelf sediments furthermore suggests that outlet glaciers had extended into coastal fjords by ~750 CE (Fig. 2c; Andrews et al., 2016). Evidence from ^{10}Be -dated moraines (Ugordleq; ULV; Fig. 2i) and glacial lake sediments (Kulusuk; Kul-10; Fig. 2h) suggests that other small glaciers rapidly advanced on S Greenland ~650–850 CE (Balascio et al., 2015; Young et al., 2015).

Previous studies have tentatively linked glacier variability in the

Arctic Atlantic to regional changes in surface ocean (sea-ice) conditions (Cabedo-Sanz et al., 2016; Larsen et al., 2013). We corroborate this by calculating significant correlations ($\rho \geq 0.5$, $p < 0.001$, $n = 74$) between selected historical glacier reconstructions from climatically-sensitive Ammassalik Island and observations of regional summer temperature and sea-ice extent since 1875 CE (Suppl. Fig. 1; Balascio et al., 2015; Divine and Dick, 2006; Morice et al., 2012; van der Bilt et al., 2018). To assess whether this coupling operated around the time of glacier reformation ~810 CE, we compare our reconstruction to well-constrained records of sea-ice and surface ocean change E of Greenland. Fig. 2d–f shows that glacier growth is coincident with rapid ocean surface cooling and the establishment of more severe seasonal sea ice conditions on the E Greenland shelf (Kolling et al., 2017; Miettinen et al., 2015; Perner et al., 2016). The magnitude of all these changes is unprecedented during the Late Holocene (past 4.2 ka) period (see stippled mean and 95% limits in Fig. 2). In keeping with the Ymer and Kulusuk glacier reconstructions, these records suggest that climate conditions tipped towards a colder mean state following rapid change (Fig. 2). By insulating the atmosphere from the exchange of Atlantic Ocean heat (Screen and Simmonds, 2010), sea ice expansion greatly amplifies surface cooling in the Arctic. We thus argue that sea-ice feedbacks best explain the magnitude and duration of Greenland climate deterioration between ~650 and 850 CE.

To assess whether the inferred coupled ocean-atmosphere-sea ice response exhibits a broader spatio-temporal pattern, we compare our findings to strategically located records of Late Holocene surface change in the Svalbard-Barents region; an area also located at the dynamic interface of Atlantic and Arctic waters near the seasonal sea-ice edge (Fig. 1). Long-term observations highlight the large amplitude of Barents sea ice variability and its substantial impact on the Arctic's surface energy budget by inhibiting heat transfer from warm Atlantic water (Smedsrød et al., 2013). Moreover, model sensitivity experiments indicate that the main conduit of Atlantic heat, the Barents Sea Inflow (BSI; Fig. 1), can shut down under CE boundary conditions in case of sea ice expansion (Lehner et al., 2013). To investigate these climate responses, we examine the only IP₂₅-based seasonal sea-ice reconstruction from the W Barents Sea that covers the entire CE (Berben et al., 2014), taken from an area near the BSI (Fig. 1). The data presented in Fig. 2b indicate that seasonal sea-ice conditions were established around 1050 CE. As on Greenland, this shift occurred in tandem with abrupt glacier growth; the XRF Ti-based reconstruction of Annabreen indicates near-synchronous reformation of the small (0.87 km^2) thus responsive Annabreen glacier on NW Spitsbergen (Fig. 2a; De Wet et al., 2017). The past years have seen many new lacustrine glacier reconstructions from Svalbard that show glacier (re)-growth ~950 CE (Bakke et al., 2018). This evidence is supported by a sharp concurrent increase in angular (glacially-derived) Ice Rafted Debris (IRD) on the western Svalbard margin (Werner et al., 2015). We specifically include the Gjøavatnet record in our compilation as the onset of glacier regrowth is constrained by a terrestrial plant-derived ^{14}C age, and decadal sampling resolution (Fig. 2a). Supporting lake-based evidence, vegetation kill dates from C Spitsbergen indicate glaciers advances after 850 CE (Humlum et al., 2005), and snowlines lowered by 60 m–1100 CE (Fig. 2i - top; Miller et al., 2017).

Combined, the collated evidence reveals a pattern of diachronous surface cooling and glacier growth ~650–950 CE from Greenland to Svalbard, which exceeded the magnitude of other Late Holocene cold events (Fig. 3). The expression and timing of this threshold response raises questions about its cause(s). We favor an atmospheric origin for the discussed shift as stable deep water flow (Thornalley et al., 2013), strengthening Sub Polar Gyre (SPG; Fig. 1) circulation (Moffa-Sánchez and Hall, 2017), and above-average



regional Sea Surface Temperatures (SSTs; Sicre et al., 2011; Spielhagen et al., 2011) indicate strong contemporaneous Atlantic Meridional Overturning Circulation (AMOC). Moreover, despite dating uncertainties and local disparities, the presented proxy compilation shows that regional climate deterioration preceded the clustered volcanic eruptions and solar minima associated with the Little Ice Age (LIA; 1250–1850 CE; Miller et al., 2012), in line with the recent composite temperature reconstruction of Werner et al. (2018). Indeed, most assessed records suggest that (maximum) change occurred during the Medieval Quiet Period (MQP; 725–1025 CE) (Fig. 2), a phase of stable radiative (volcanic, solar) forcing (Bradley et al., 2016).

The spatio-temporal signature of reconstructed change also discounts radiative forcing as the most plausible explanation. Observations and simulations both indicate that the impact of volcanic eruptions and solar minima affects surface conditions synchronously across the North Atlantic Arctic (Moffa-Sánchez et al., 2014; Slawinska and Robock, 2017). In contrast, the presented proxy evidence reveals a diachronous pattern. For example, based on the computed timing of maximum change (methods), cooling on Svalbard lags by at least ~20 yrs, but most likely ~230 yrs (Fig. 2). Following from the above, we argue that the timing and pattern of reconstructed change preclude two often invoked external forcings of CE cooling – volcanic eruptions and solar minima.

Recent climate model experiments indicate that abrupt coupled Arctic Atlantic surface temperature and sea ice shifts may arise without forcing under CE (pre-industrial) conditions (Drijfhout et al., 2013; Kleppin et al., 2015). Could the investigated threshold response have emerged spontaneously (unforced)? To examine this hypothesis, we analyze a pre-industrial control run from the coupled EC-Earth 2.2 climate model (Methods; Hazeleger et al., 2012). This simulation replicates key features of our proxy synthesis by revealing a rapid surface cooling pattern that emerges over SE Greenland between 390 and 410 years into the run (Fig. 3a), before extending towards Svalbard.

It also provides a mechanism of abrupt change by showing that the onset of surface cooling over Greenland is coincident with the establishment of a positive Sea Level Pressure (SLP) anomaly over the eastern Subpolar Gyre (SPG) (Fig. 3a). This anti-cyclonic circulation pattern is not persistent, but the integrated result of an increased number of blocking highs as outlined by Drijfhout et al. (2013). Such events enhance surface heat loss by suppressing cloud formation and weakening westerly winds over Greenland,

Fig. 2. Collated proxy evidence for CE Arctic Atlantic glacier-climate change (locations in Fig. 1 with matching colors). **A:** The Ti-based Annabreen glacier reconstruction from Gjøavatnet on NW Spitsbergen (De Wet et al., 2017), showing raw values (light) and 30-year averages (dark). **B:** IP₂₅-derived seasonal sea ice conditions on the W Barents Sea (Berben et al., 2014). **C:** Glacier-derived mineral fraction in E Greenland fjords (Andrews et al., 2016). **D:** IP₂₅-derived seasonal sea ice conditions on the E Greenland shelf (Kolling et al., 2017). **E:** Cold foraminifera abundances on the E Greenland shelf (Perner et al., 2016). **F:** Raw (grey) and 5-point averages (red) of *Fragilariaopsis* diatom-derived sea ice severity (melt rates) on the SE Greenland shelf (Miettinen et al., 2015). **G:** Non-glacial (yellow) and glaciogenic (blue) grain size signatures in E Greenland Ymer Lake sediments (van der Bilt et al., 2018). **H:** Raw (grey) and 30-year averages (black) of the XRF PC1-based reconstruction from Kulusuk glacier (Balascio et al., 2015). **I:** Cumulative (n samples) vegetation kill (green) and moraine (red) ages that date glacier advances in S Greenland. Sources: W Greenland (WGM; Schweinsberg et al., 2017), Mittivakkat (MT; Hasholt, 2000), Istortvet (IST; Lowell et al., 2013; Miller et al., 2013), Uigordleq Lake Valley (ULV; Young et al., 2015), and Jotunfonna (JOF; Miller et al., 2017). For all sediment records, we show mean values (black stippled) and standard deviations (red stippled) of data from the foregoing Late Holocene period (4.2–1.5 ka BP). We highlight the calibrated distribution of dates closest to periods of maximum change (methods). These intervals are marked by vertical bars, as well as dashed (95%) and solid (means) lines. Mild (MQP; Medieval Quiet Period, MWP; Medieval Warm Period, 825–1025 CE) and cold (LIA; Little Ice Age, 1250–1850 CE) events are accentuated with red and blue bars. (For interpretation of the references to color in this figure legend, the reader is referred to the Web version of this article.)

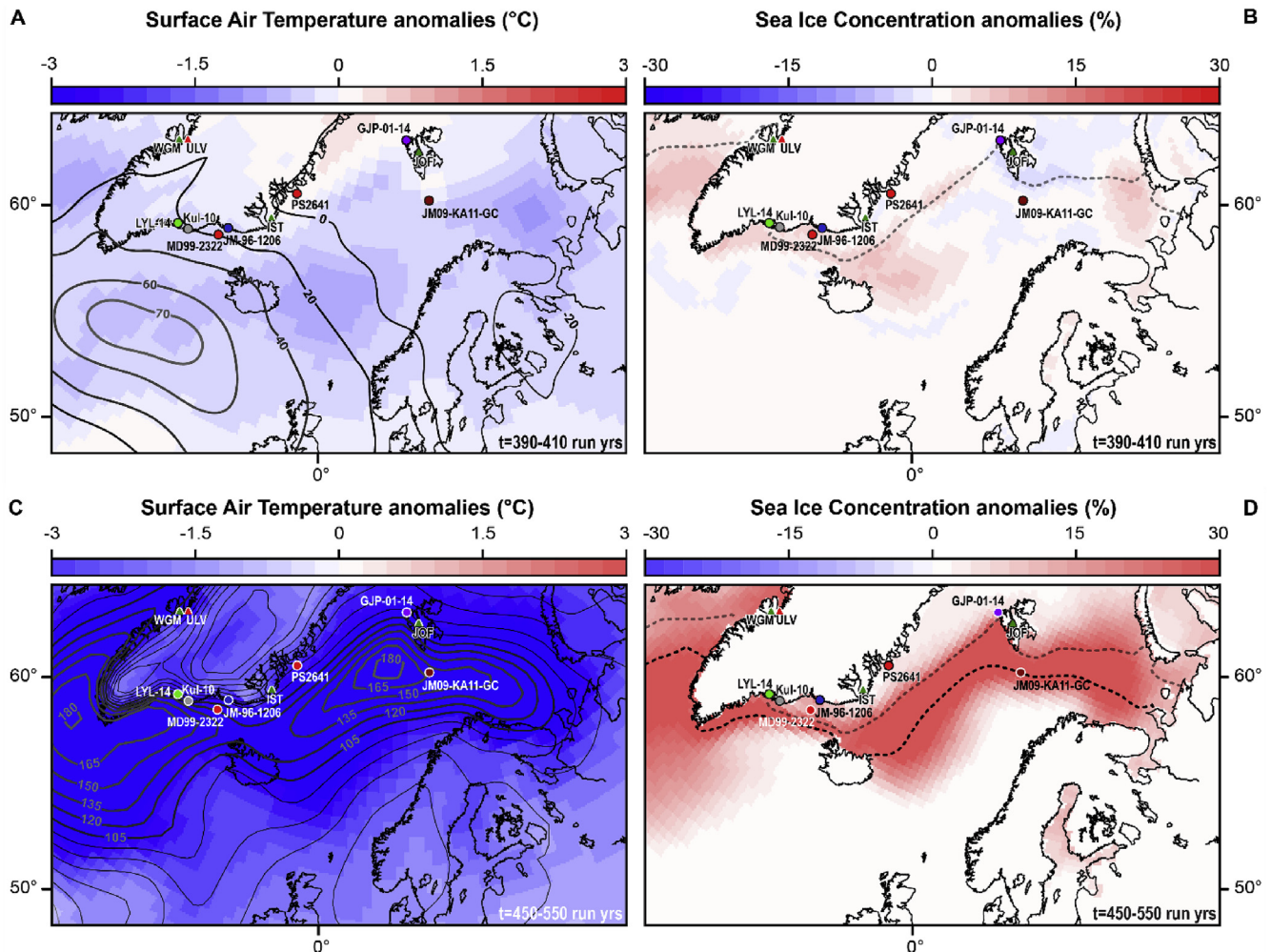


Fig. 3. Modeled unforced PI change. Anomalies in Surface Air Temperature (SAT; °C), Sea Level Pressure (SLP; Pa isobars), and Sea Ice Concentrations (SIC), between the onset (390–410 years) (A, B), and culmination (450–550 years) of the analyzed cold event (C, D). We express anomalies against a reference climate state (200–390 years) after Drijfhout et al. (2013). For context, we highlight discussed proxy records with colors matching Figs. 1–2. The sea-ice margin (min. 50% annual coverage) is delineated in grey (reference climate) and black (cold event). (For interpretation of the references to color in this figure legend, the reader is referred to the Web version of this article.)

while drawing in Arctic air. Surface Air Temperatures (SAT) thereupon decline as Sea Ice Concentrations (SIC) increase (Fig. 3b). As the prime control on regional ocean to atmosphere heat exchange (Screen and Simmonds, 2010), sea ice expansion enables positive SAT and SLP anomalies to expand by cooling and compressing overlying air, respectively. Within 40 run years, this feedback mechanism allowed coupled SAT-SIC-SLP anomalies to strengthen and expand across the Arctic Atlantic towards Svalbard, culminating between 450 and 550 years into the run (Fig. 3c and d). The findings of Kleppin et al. (2015) bolster the robustness of the outlined mechanism by detecting the same atmospheric trigger in a pre-industrial control run of another recent coupled climate model (CCSM 4). In conclusion, we contend that stochastic atmospheric change, excited by sea-ice feedbacks, tipped Arctic Atlantic climate towards a colder mean state around 650–950 CE.

Acknowledgements

We extend our gratitude to Johannes Werner for his statistical advice, and Jordan Donn Holl for her assistance with sediment analyses. This work was supported by an EU-Interact TA grant (GLEESP). AB and KA are supported by starting grants from the

Trond Mohn Foundation. Finally, we thank Anne Hormes and one anonymous reviewer for improving this manuscript.

Appendix A. Supplementary data

Supplementary data to this article can be found online at <https://doi.org/10.1016/j.quascirev.2019.07.042>.

References

- Andresen, C.S., Straneo, F., Rønne, M.H., Bjørk, A.A., Andersen, T.J., Kuijpers, A., Nørgaard-Pedersen, N., Kjær, K.H., Schjøth, F., Weckström, K., 2012. Rapid response of Helheim Glacier in Greenland to climate variability over the past century. *Nat. Geosci.* 5, 37–41.
- Andrews, J.T., Stein, R., Moros, M., Perner, K., 2016. Late Quaternary changes in sediment composition on the NE Greenland margin (~73° N) with a focus on the fjords and shelf. *Boreas* 45, 381–397.
- Bahr, D.B., Pfeffer, W.T., Sassolas, C., Meier, M.F., 1998. Response time of glaciers as a function of size and mass balance: 1. Theory. *J. Geophys. Res. Solid Earth* 103, 9777–9782.
- Bakke, J., Balascio, N., van der Bilt, W.G., Bradley, R., D'Andrea, W.J., Gjerde, M., Ólafsdóttir, S., Røthe, T., De Wet, G., 2018. The Island of Amsterdamoya: a key site for studying past climate in the Arctic Archipelago of Svalbard. *Quat. Sci. Rev.* 183, 157–163.
- Bakke, J., Lie, Ø., Heegaard, E., Dokken, T., Haug, G.H., Birks, H.H., Dulski, P., Nilsen, T., 2009. Rapid oceanic and atmospheric changes during the Younger Dryas cold

- period. *Nat. Geosci.* 2, 202–205.
- Balscino, N.L., D'Andrea, W.J., Bradley, R., 2015. Glacier response to North Atlantic climate variability during the Holocene. *Clim. Past* 11, 1587–1598.
- Berben, S., Husum, K., Cabedo-Sanz, P., Belt, S.T., 2014. Holocene sub-centennial evolution of Atlantic water inflow and sea ice distribution in the western Barents Sea. *Clim. Past* 10, 181–198.
- Bernhardt, A., Schwanghart, W., Hebbeln, D., Stuut, J.-B.W., Strecker, M.R., 2017. Immediate propagation of deglacial environmental change to deep-marine turbidite systems along the Chile convergent margin. *Earth Planet. Sci. Lett.* 473, 190–204.
- Bevan, A., Crema, E.R., Silva, F., 2018. Carbon v1.2.0: Methods for Calibrating and Analysing Radiocarbon Dates.
- Björk, A.A., Kjær, K.H., Korsgaard, N.J., Khan, S.A., Kjeldsen, K.K., Andresen, C.S., Larsen, N.K., Funder, S., 2012. An aerial view of 80 years of climate-related glacier fluctuations in southeast Greenland. *Nat. Geosci.* 5, 427–432.
- Bradley, R.S., Wanner, H., Diaz, H.F., 2016. The medieval quiet period. *Holocene* 26, 990–993.
- Cabedo-Sanz, P., Belt, S.T., Jennings, A.E., Andrews, J.T., Geirsdóttir, A., 2016. Variability in drift ice export from the Arctic Ocean to the North Icelandic Shelf over the last 8000 years: a multi-proxy evaluation. *Quat. Sci. Rev.* 146, 99–115.
- De Wet, G., Balscino, N.L., D'Andrea, W.J., Bakke, J., Bradley, R.S., Perren, B., 2017. Holocene glacier activity reconstructed from proglacial lake Gjøavatnet on Amsterdamøya, NW Svalbard. *Quat. Sci. Rev.* 183, 188–203.
- Divine, D.V., Dick, C., 2006. Historical variability of sea ice edge position in the Nordic Seas. *J. Geophys. Res.: Oceans* 111.
- Drijfhout, S., Gleeson, E., Dijkstra, H.A., Livina, V., 2013. Spontaneous abrupt climate change due to an atmospheric blocking–sea-ice–ocean feedback in an unforced climate model simulation. *Proc. Natl. Acad. Sci.* 110, 19713–19718.
- Fetterer, F., Knowles, K., Meier, W., Savoie, M., 2016. In: Center, N.N.S.a.I.D (Ed.), Sea Ice Index, Version 2, 2 ed. Boulder, Colorado (USA).
- Hasholt, B., 2000. Evidence of a warmer climate around AD 600, Mittivakkat glacier, South east Greenland. *Geografisk Tidsskrift* 100.
- Hazeleger, W., Wang, X., Severijns, C., Štefánescu, S., Bintanja, R., Sterl, A., Wyser, K., Semmler, T., Yang, S., Van den Hurk, B., 2012. EC-Earth V2. 2: description and validation of a new seamless earth system prediction model. *Clim. Dyn.* 39, 2611–2629.
- Hormes, A., Beer, J., Schlüchter, C., 2006. A geochronological approach to understanding the role of solar activity on Holocene glacier length variability in the Swiss Alps. *Geogr. Ann. Ser. A Phys. Geogr.* 88, 281–294.
- Humlum, O., Elberling, B., Hormes, A., Fjordheim, K., Hansen, O.H., Heinemeier, J., 2005. Late-Holocene glacier growth in Svalbard, documented by subglacial relict vegetation and living soil microbes. *Holocene* 15, 396–407.
- IPCC, 2001. Climate Change 2001: The Scientific Basis: Part of the Working Group I Contribution to the Third Assessment Report of the Intergovernmental Panel on Climate Change. IPCC.
- Kleppin, H., Jochum, M., Otto-Bliesner, B., Shields, C.A., Yeager, S., 2015. Stochastic atmospheric forcing as a cause of Greenland climate transitions. *J. Clim.* 28, 7741–7763.
- Kolling, H.M., Stein, R., Fahl, K., Perner, K., Moros, M., 2017. Short-term variability in late Holocene sea ice cover on the East Greenland Shelf and its driving mechanisms. *Palaeogeogr. Palaeoclimatol. Palaeoecol.* 485, 336–350.
- Larsen, D.J., Miller, G.H., Geirsdóttir, Á., 2013. Asynchronous little ice age glacier fluctuations in Iceland and European Alps linked to shifts in subpolar North Atlantic circulation. *Earth Planet. Sci. Lett.* 380, 52–59.
- Larsen, N.K., Strunk, A., Levy, L.B., Olsen, J., Bjørk, A., Lauridsen, T.L., Jeppesen, E., Davidson, T.A., 2017. Strong altitudinal control on the response of local glaciers to Holocene climate change in southwest Greenland. *Quat. Sci. Rev.* 168, 69–78.
- Leemann, A., Niessen, F., 1994. Varve formation and the climatic record in an Alpine proglacial lake: calibrating annually-laminated sediments against hydrological and meteorological data. *Holocene* 4, 1–8.
- Lehner, F., Born, A., Raible, C.C., Stocker, T.F., 2013. Amplified inception of European Little Ice Age by sea ice–ocean–atmosphere feedbacks. *J. Clim.* 26, 7586–7602.
- Levy, L.B., Kelly, M.A., Lowell, T.V., Hall, B.L., Hempel, L.A., Honsaker, W.M., Lusas, A.R., Howley, J.A., Axford, Y.L., 2014. Holocene fluctuations of Bregne ice cap, Scoresby Sund, east Greenland: a proxy for climate along the Greenland Ice Sheet margin. *Quat. Sci. Rev.* 92, 357–368.
- Liu, Z., Zhu, J., Rosenthal, Y., Zhang, X., Otto-Bliesner, B.L., Timmermann, A., Smith, R.S., Lohmann, G., Zheng, W., Timm, O.E., 2014. The Holocene temperature conundrum. *Proc. Natl. Acad. Sci.* 111, E3501–E3505.
- Lowell, T.V., Hall, B.L., Kelly, M.A., Bennike, O., Lusas, A.R., Honsaker, W., Smith, C.A., Levy, L.B., Travis, S., Denton, G.H., 2013. Late Holocene expansion of Istorvet ice cap, Liverpool Land, east Greenland. *Quat. Sci. Rev.* 63, 128–140.
- Mann, M.E., Zhang, Z., Rutherford, S., Bradley, R.S., Hughes, M.K., Shindell, D., Ammann, C., Faluvegi, G., Ni, F., 2009. Global signatures and dynamical origins of the little ice age and medieval climate anomaly. *Science* 326, 1256–1260.
- McKay, N.P., Kaufman, D.S., Routson, C.C., Erb, M.P., Zander, P.D., 2018. The onset and rate of Holocene Neoglacial cooling in the Arctic. *Geophys. Res. Lett.* 45 (12), 487–412,496.
- Miettinen, A., Divine, D.V., Husum, K., Koç, N., Jennings, A., 2015. Exceptional ocean surface conditions on the SE Greenland shelf during the Medieval Climate Anomaly. *Paleoceanography* 30, 1657–1674.
- Miller, G.H., Briner, J.P., Refsnider, K.A., Lehman, S.J., Geirsdóttir, Á., Larsen, D.J., Southon, J.R., 2013. Substantial agreement on the timing and magnitude of Late Holocene ice cap expansion between East Greenland and the Eastern Canadian Arctic: a commentary on Lowell et al., 2013. *Quat. Sci. Rev.* 77, 239–245.
- Miller, G.H., Geirsdóttir, Á., Zhong, Y., Larsen, D.J., Otto-Bliesner, B.L., Holland, M.M., Bailey, D.A., Refsnider, K.A., Lehman, S.J., Southon, J.R., 2012. Abrupt onset of the Little Ice Age triggered by volcanism and sustained by sea-ice/ocean feedbacks. *Geophys. Res. Lett.* 39.
- Miller, G.H., Landvik, J.Y., Lehman, S.J., Southon, J.R., 2017. Episodic Neoglacial snowline descent and glacier expansion on Svalbard reconstructed from the 14 C ages of ice-entombed plants. *Quat. Sci. Rev.* 155, 67–78.
- Moffa-Sánchez, P., Born, A., Hall, I.R., Thornalley, D.J., Barker, S., 2014. Solar forcing of North Atlantic surface temperature and salinity over the past millennium. *Nat. Geosci.* 7, 275–278.
- Moffa-Sánchez, P., Hall, I.R., 2017. North Atlantic variability and its links to European climate over the last 3000 years. *Nat. Commun.* 8, 1726.
- Morice, C.P., Kennedy, J.J., Rayner, N.A., Jones, P.D., 2012. Quantifying uncertainties in global and regional temperature change using an ensemble of observational estimates: the HadCRUT4 data set. *J. Geophys. Res. Atmos.* 117.
- Perner, K., Jennings, A.E., Moros, M., Andrews, J.T., Wacker, L., 2016. Interaction between warm Atlantic-sourced waters and the East Greenland Current in northern Denmark Strait (68° N) during the last 10 600 cal a BP. *J. Quat. Sci.* 31, 472–483.
- Philips, W., Briner, J., Gislefoss, L., Linge, H., Koffman, T., Fabel, D., Xu, S., Hormes, A., 2017. Late Holocene glacier activity at inner Hornsund and Scottbreen, southern Svalbard. *J. Quat. Sci.* 32, 501–515.
- Schweinsberg, A.D., Briner, J.P., Miller, G.H., Bennike, O., Thomas, E.K., 2017. Local glaciation in west Greenland linked to North Atlantic ocean circulation during the Holocene. *Geology* 45, 195–198.
- Screen, J.A., Simmonds, I., 2010. The central role of diminishing sea ice in recent Arctic temperature amplification. *Nature* 464, 1334–1337.
- Sicre, M.A., Hall, I.R., Mignot, J., Khodri, M., Ezat, U., Truong, M.X., Eiríksson, J., Knudsen, K.L., 2011. Sea surface temperature variability in the subpolar Atlantic over the last two millennia. *Paleoceanography* 26.
- Slawinska, J., Robock, A., 2017. Impact of volcanic eruptions on decadal to centennial fluctuations of Arctic sea ice extent during the last millennium and on initiation of the little ice age. *J. Clim.* 31 (6).
- Smedsrød, L.H., Esau, I., Ingvaldsen, R.B., Eldevik, T., Haugan, P.M., Li, C., Lien, V.S., Olsen, A., Omar, A.M., Otterå, O.H., 2013. The role of the Barents Sea in the Arctic climate system. *Rev. Geophys.* 51, 415–449.
- Solomina, O.N., Bradley, R.S., Jomelli, V., Geirsdóttir, A., Kaufman, D.S., Koch, J., McKay, N.P., Masiokas, M., Miller, G., Nesje, A., Nicolussi, K., Owen, L.A., Putnam, A.E., Wanner, H., Wiles, G., Yang, B., 2016. Glacier fluctuations during the past 2000 years. *Quat. Sci. Rev.* 149, 61–90.
- Spillhaugen, R.F., Werner, K., Sørensen, S.A., Zamelczyk, K., Kandiano, E., Budeus, G., Husum, K., Marchitto, T.M., Hald, M., 2011. Enhanced modern heat transfer to the Arctic by warm Atlantic water. *Science* 331, 450–453.
- Straneo, F., Hamilton, G.S., Sutherland, D.A., Stearns, L.A., Davidson, F., Hammill, M.O., Stenson, G.B., Rosing-Asvid, A., 2010. Rapid circulation of warm subtropical waters in a major glacial fjord in East Greenland. *Nat. Geosci.* 3, 182–186.
- Thornalley, D.J., Blaschek, M., Davies, F.J., Praetorius, S., Oppo, D.W., McManus, J.F., Hall, I.R., Kleiven, H.F., Renssen, H., McCave, I.N., 2013. Long-term Variations in Iceland–Scotland Overflow Strength during the Holocene.
- van der Bilt, W.G., Rea, B., Spagnolo, M., Roerdink, D., Jorgensen, S., Bakke, J., 2018. Novel sedimentological fingerprints link shifting depositional processes to Holocene climate transitions in East Greenland. *Glob. Planet. Chang.* 164.
- van der Bilt, W.G.M., Bakke, J., Vasskog, K., D'Andrea, W.J., Bradley, R.S., Ólafsdóttir, S., 2015. Reconstruction of glacier variability from lake sediments reveals dynamic Holocene climate in Svalbard. *Quat. Sci. Rev.* 126, 201–218.
- Werner, J.P., Divine, D.V., Ljungqvist, F.C., Nilsen, T., Francus, P., 2018. Spatio-temporal variability of Arctic summer temperatures over the past 2 millennia. *Clim. Past* 14, 527.
- Werner, K., Müller, J., Husum, K., Spielhagen, R.F., Kandiano, E.S., Polyak, L., 2015. Holocene sea subsurface and surface water masses in the Fram Strait—Comparisons of temperature and sea-ice reconstructions. *Quat. Sci. Rev.* 147, 194–209.
- Young, N.E., Schweinsberg, A.D., Briner, J.P., Schaefer, J.M., 2015. Glacier maxima in Baffin Bay during the medieval Warm Period coeval with Norse settlement. *Sci. Adv.* 1, e1500806.